

Excitation of dynamic chaos in a monolithic ring chip laser upon periodic modulation of mechanical stresses in the active element

N.V. Kravtsov, S.S. Sidorov, P.P. Pashinin, V.V. Firsov, S.N. Chekina

Abstract. The peculiarities of nonlinear dynamics of solid-state bidirectional ring Nd : YAG chip lasers are studied theoretically and experimentally during periodic modulation of mechanical stresses in the active element. It is shown that modulation of mechanical stresses is an effective method for exciting dynamic chaos in a monolithic chip laser.

Keywords: ring laser, nonlinear dynamics, dynamic chaos.

1. Introduction

A considerable attention has been devoted in recent years to the study of nonlinear self-sustained oscillatory processes and dynamic chaos in solid-state lasers. Such investigations are undoubtedly interesting for the development of laser physics as well as for solving a number of applied problems. In these investigations, the main attention is focused on the conditions of emergence of dynamic chaos in optically coupled single-mode lasers [1–5], in lasers emitting orthogonally polarised modes [6–9], as well as in ring lasers [10–13].

The most interesting (and, in our opinion, the most complex) objects of investigation among the ones mentioned above are bidirectional ring lasers. It is well known that solid-state ring lasers have a quite complex nonlinear dynamics due to competing interaction of counterpropagating waves in the active medium at the induced inverse population grating and their coupling through backward scattering. This leads to a variety of lasing regimes in such lasers, including various specific self-sustained oscillatory processes. The amplitude and frequency nonreciprocities in ring cavities play an important role in a variety of lasing regimes in ring lasers [14, 15].

Dynamic chaos regimes are among the most interesting lasing regimes existing in solid-state bidirectional ring lasers. As a rule, such regimes are excited during external modulation of laser parameters. In the absence of external modulation, the dynamic chaos regimes may emerge in a

bidirectional ring laser under parametric resonance conditions [16]. However, in contrast to nonautonomous lasers, the realisation of such regimes in autonomous ring lasers is often found to be quite difficult. Some features of chaotic oscillations are also observed upon excitation of self-modulation regimes of second kind [17].

Detailed investigations of nonlinear dynamics are possible only for a high stability of parameters of the laser under study. High stability of parameters is attained quite easily in a thermally stabilised monolithic ring chip laser pumped by a semiconductor laser. Because intracavity control elements cannot be used in such a laser, the possibilities to control its operating regimes are considerably restricted. The pump power is the only controlling parameter used in almost all experimental studies of the nonlinear dynamics of monolithic ring chip lasers. The use of an alternating magnetic field as a control parameter is hampered by the difficulties in obtaining high field strengths at high (100–200 kHz) frequencies.

In this work, we studied yet another possibility of exciting quasi-periodic and chaotic lasing regimes in monolithic ring chip lasers, which is based on the modulation of mechanical stresses in the active element of the laser. A periodic variation in mechanical stresses leads to a simultaneous modulation of several parameters of the laser, including the refractive index of the active element, lasing frequency detuning from the centre of the gain line, the cavity length, as well as the cavity losses caused by birefringence in the polarisation-anisotropic cavity. Our investigations showed that in this case, modulation of the last of the above parameters affects lasing most significantly.

2. Experimental setup

The experimental setup is shown schematically in Fig. 1. Highly stable monolithic ring 1.06- μm Nd : YAG chip laser (1) pumped by a semiconductor laser was investigated. The perimeter of the ring laser cavity was 2.6 cm, and the nonflatness angle was 80°. The laser was pumped longitudinally by 0.81- μm laser diode (2) with an output power up to 0.5 W. The laser design is described in detail in Ref. [18].

The crystal of the chip laser was rigidly connected to piezoceramic plate (3) and placed in a metal housing. An alternating voltage from generator (4) was applied to the piezoelement. The self-modulation frequency $\omega_m/2\pi$ and the fundamental relaxation frequency $\omega_r/2\pi$ could be varied within a narrow range by adjusting the active element with

N.V. Kravtsov, V.V. Firsov, S.N. Chekina D.V. Skobel'tsyn Institute of Nuclear Physics, M.V. Lomonosov Moscow State University, Vorob'evy gory, 119992 Moscow, Russia;

S.S. Sidorov, P.P. Pashinin A.M. Prokhorov General Physics Institute, Russian Academy of Sciences, ul. Vavilova 38, 119991 Moscow, Russia

Received 1 December 2003

Kvantovaya Elektronika 34 (4) 329–332 (2004)

Translated by Ram Wadhwa

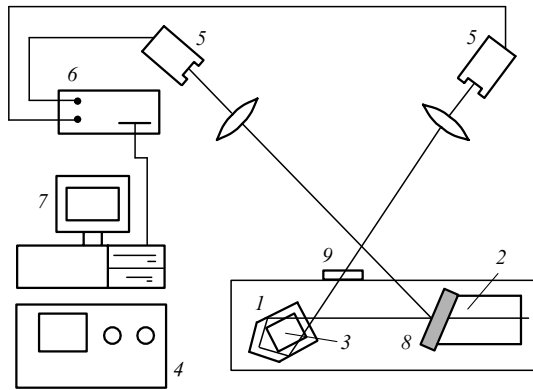


Figure 1. Scheme of the setup: (1) monolithic ring chip laser; (2) semiconductor laser diode; (3) piezoelement; (4) ac voltage generator; (5) LFD-2 photodetector; (6) ACK-3151 digital oscilloscope; (7) computer; (8) selective mirror; (9) IKS optical filter.

respect to the pump-beam axis. The voltage U across the piezoelement (which was varied from 0 to 20 V) determined the modulation depth h of mechanical stresses in the active element. Modulation was performed in the frequency range from $\omega_p/2\pi = 10$ to 160 kHz. The laser radiation was incident on LFD-2 photodetector (5), whose output signal was fed to ACK-3151 digital oscilloscope (6) and processed with computer (7). Temporal and spectral characteristics of counterpropagating waves of the bidirectional solid-state ring laser were recorded during the experiment. Projections of phase portraits were obtained by processing the experimental results.

3. Experimental results

We studied the evolution of lasing regimes in a monolithic ring Nd : YAG chip laser by varying mechanical stresses in the active element and the scenario of transition to the dynamic chaos. In the absence of modulation ($U = 0$), the laser operates in the self-modulation lasing regime of the first kind typical of a ring laser. The counterpropagating waves had the same intensity and their spectrum consisted of a single component with a self-modulation frequency $\omega_m/2\pi = 145$ kHz, while the fundamental relaxation frequency was $\omega_r/2\pi = 65$ kHz above the pump threshold $\eta = 0.16$.

When the control ac voltage ($U \neq 0$) was applied to the piezoelement, quasi-sinusoidal oscillations were excited, and the envelopes of intensities of counterpropagating waves were modulated in turn at the frequency $\omega_p/2\pi$, and an additional component with the same frequency appeared in the spectrum. As the voltage U (i.e., the modulation depth) increased up to a certain critical value U_{cr} , the quasi-periodic oscillations transformed to the dynamic chaos regime. When the circular modulation frequency ω_p satisfied the parametric resonance condition $\omega_m = \omega_r + \omega_p$ (where k, m, n are integers), the control voltage U_{cr} across the piezoelement was minimal.

We found in experiments that switching of lasing regimes and transition to chaotic oscillations occur most easily (i.e., for the lower modulation depth) in the frequency range $60 < \omega_p/2\pi < 90$ kHz, which is apparently, due to the presence of resonance frequencies for the crystal–piezoelement–housing system in this frequency range, making it

possible to realise quite easily the condition of fundamental parametric resonance $\omega_m = \omega_r + \omega_p$ ($\omega_m = 145$ kHz, $\omega_p = 80$ kHz, $\omega_r = 65$ kHz), where $\omega_i = \omega_i/2\pi$, $i = m, r, p$. The minimum value of the voltage U_{cr} across the piezoelement at which dynamic chaos appears is 3 V for this frequency range.

Figure 2 shows the oscillograms of intensities $I_{1,2}(t)$, the spectra of counterpropagating waves and the phase portrait in the (I_1, I_2) plane under parametric resonance conditions $\omega_m = \omega_r + \omega_p$ and for $\eta = 0.16$, $U = 15$ V. One can see that the time dependences of the intensities of counterpropagating waves are trains of peaks with chaotically varying amplitudes and time intervals between them. The coefficient K of correlation between intensities of counterpropagating waves is equal to 0.43 in this case. The emission spectra of counterpropagating waves are nearly continuous with maxima at frequencies ω_r, ω_p and ω_m . We found that the width of the parametric resonance region is proportional to the modulation depth of mechanical stresses, and is ~ 3 kHz and ~ 6 kHz for control voltage $U = 5$ and 15 V, respectively, for the laser whose oscillograms are shown in Fig. 2. The obtained results [temporal characteristics, emission spectra and the projection of the phase trajectory on the (I_1, I_2) plane] indicate that the dynamic chaos is excited in a ring laser.

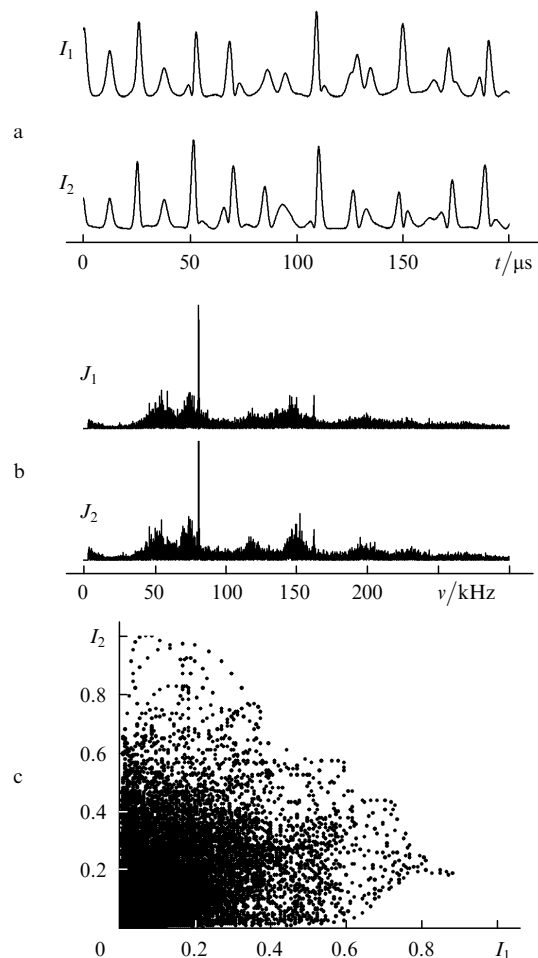


Figure 2. (a) Oscillograms of intensities I_1, I_2 of counterpropagating waves, (b) their spectra, and (c) phase trajectory projection on the I_1, I_2 plane, in the case of parametric resonance $\omega_m = \omega_r + \omega_p$ for $\omega_m = 145$ kHz, $\omega_p = 80$ kHz, $\omega_r = 65$ kHz, $\eta = 0.16$, and $U = 15$ V.

Figure 3 shows the scenario of transition to the dynamic chaos for $\nu_m = 165$ kHz, $\nu_p = 84$ kHz, $\nu_r = 84$ kHz, and $\eta = 0.4$. It presents the oscillograms of radiation intensities for one of the counterpropagating waves, by varying the control parameter (increasing U), and the corresponding spectra. One can see that as the voltage increases, the harmonic oscillation regime is first replaced by a quasi-periodic regime, which becomes unstable as the voltage attains the critical value U_{cr} , and is transformed into the dynamic chaos regime. Such an evolution of lasing regimes is called quasi-periodic (Ruelle–Tuckens) scenario of transition to chaos (see, for example, Ref. [19]). Note that such a scenario was observed in Ref. [20].

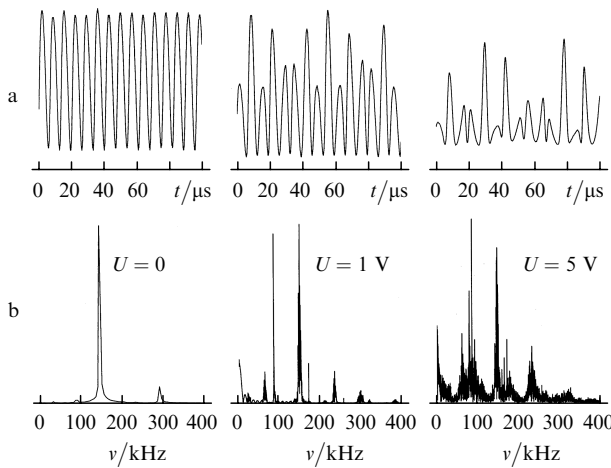


Figure 3. Dependence of temporal (a) and the corresponding spectral characteristics (b) of one of the counterpropagating waves in a ring chip laser on the control parameter (voltage across the piezoelement) for $\nu_m = 165$ kHz, $\nu_p = 84$ kHz, $\nu_r = 84$ kHz, and $\eta = 0.4$.

4. Numerical simulation

Calculations were carried out using the standard model of a solid-state ring laser described by the system of equations [21]:

$$\frac{dE_{1,2}}{dt} = -\frac{\omega}{2Q} E_{1,2} + \frac{im}{2} E_{2,1} + \frac{\sigma L}{2T} (N_0 E_{1,2} + N_{\pm} E_{2,1}),$$

$$T_1 \frac{dN_0}{dt} = N_{th}(1 + \eta) - N_0 [1 + a(|E_1|^2 + |E_2|^2)]$$

$$-a(N_+ E_1 E_2^* + N_- E_1^* E_2),$$

$$T_1 \frac{dN_{\pm}}{dt} = -N_{\pm} [1 + a(|E_1|^2 + |E_2|^2)] - aN_0 E_1 E_2^*,$$

$$N_0 = \frac{1}{L} \int_0^L N dz, \quad N_{\pm} = \frac{1}{L} \int_0^L N \exp(\pm i2kz) dz, \quad N_- = N_+^*,$$

where N_{th} is the threshold inversion population density; ω is the optical lasing frequency of the chip laser; Q is the Q factor of the resonator; m is the coupling coefficient of counterpropagating waves; L is the geometrical length (perimeter) of the ring resonator; $T = nL/c$ is the transit time for light in the resonator; n is the refractive index of

the active medium; η is the excess of the pump power over the threshold; σ is the resonance transition cross section; and a is the saturation parameter.

The width ρ of the resonator band can be written in the form

$$\rho = \frac{\omega}{Q} = \frac{1-R}{T},$$

where $1-R$ are the intracavity losses. Mechanical stresses in the active element of the laser lead to the emergence of birefringence in an isotropic crystal. In the case of an anisotropic resonator, this causes additional losses for the lasing mode. Modulation of mechanical stresses with the help of a piezoelement results in a variation of T as well as R (analysis shows that the variation in R is much more significant than in T). Hence, we obtain for the case under study

$$\rho = \rho_0(1 + h \cos \omega_p t),$$

where ρ_0 is the resonator band width in the absence of modulation.

Calculations were performed assuming that the coupling coefficients of counterpropagating waves are complex conjugated. It was also assumed that the lasing frequency ω coincides with the centre ω_0 of the gain line. Earlier investigations of the self-modulation regime showed that these assumptions are well satisfied for real ring chip lasers: the coupling coefficients in monolithic chip lasers are close to their complex conjugates, and the relative detuning of the lasing frequency is small, as a rule.

Numerical simulation was carried out using the parameters of the experimentally investigated ring chip laser. The modulation frequency $\nu_p = 80$ kHz was selected, and the modulation depth h was varied from $2 \times 10^{-2} \%$ to $8 \times 10^{-2} \%$. Unfortunately, the dependence $h(U)$ could not be measured with a high precision in the experiments. Calculations show that the best agreement with the experiments is attained for $h = 5 \times 10^{-2} \%$.

Figure 4 shows the time dependences and spectra of counterpropagating waves calculated for $\nu_m = 145$ kHz, $\nu_p = 84$ kHz, $\nu_r = 64$ kHz, $\eta = 0.16$, and $h = 5 \times 10^{-2} \%$. These parameters are close to the experimental values (see Fig. 2). One can see that the results of numerical simulation are in fairly good agreement with experiments.

5. Conclusions

Our experimental studies have shown that lasing regimes can be switched from one mode to another and dynamic chaos can be excited in a monolithic ring chip laser by modulating mechanical stresses in the active element. It is shown that a transition to the dynamic chaos occurs according to the Ruelle–Tuckens scenario. A comparison of the experimental results with the results of numerical simulation based on the standard model of a solid-state ring laser leads to the conclusion that the main physical mechanism responsible for the emergence of nonstationary lasing regimes is the modulation of resonator losses during the modulation of mechanical stresses in the active element of the laser.

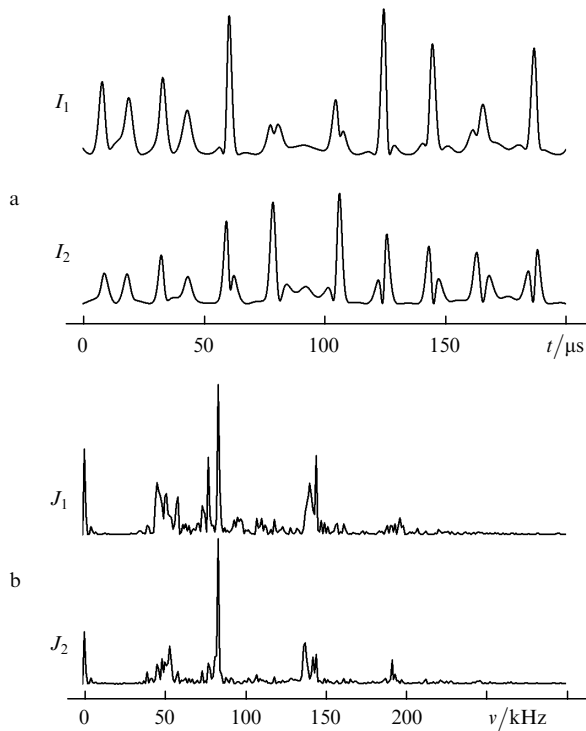


Figure 4. Calculated characteristics of a ring chip laser: (a) intensities I_1 , I_2 of counterpropagating waves, and (b) their spectra for $\nu_m = 145$ kHz, $\nu_p = 84$ kHz, $\nu_r = 64$ kHz, $\eta = 0.16$, and $h = 5 \times 10^{-2}$ %.

Acknowledgements. The authors thank E.G. Larionov for useful discussions of the problem investigated in this work. This work was supported by the Russian Foundation for Basic Research (Grant No. 02-02-16391).

References

- [doi>](#) 1. Roy R., Thornburg K.S. *Phys. Rev. Lett.*, **72**, 2009 (1994).
- [doi>](#) 2. Thornburg K.S., Moller M., Roy R. *Phys. Rev. E*, **55**, 3865 (1997).
- [doi>](#) 3. Uchida A., Sato N., Takeoka M., Kannari F. *Jpn. J. Appl. Phys.*, **36**, 912 (1997).
- [doi>](#) 4. Uchida A., Ogawa T., Shinozuka M., Kannari F. *Phys. Rev. E*, **62**, 1960 (2000).
- [doi>](#) 5. De Shazer D., Breban R., Ott E., Roy E. *Phys. Rev. Lett.*, **87**, 044101(4) (2001).
- [doi>](#) 6. Dalglish R., May A.D., Stephan G. *IEEE J. Quantum Electron.*, **34**, 1485 (1998); *IEEE J. Quantum Electron.*, **34**, 1493 (1998).
- [doi>](#) 7. Brunel M., Emile O., Alouini M., Le Floch A., Bretenaker F. *Phys. Rev. A*, **59**, 831 (1999).
8. Besnard P., Xiaolin J., Dalglish R., May A.D., Stephan G. *J. Opt. Soc. Am. B*, **10**, 1605 (1993).
9. Khandokhin P.A., Khanin Ya.I. *Kvantovaya Elektron.*, **11**, 1483 (1984) [*Sov. J. Quantum Electron.*, **14**, 1004 (1984)].
- [doi>](#) 10. Zolotoverkh I.I., Kravtsov N.V., Lariontsev E.G. *Kvantovaya Elektron.*, **22**, 213 (1995) [*Quantum Electron.*, **25**, 197 (1995)].
- [doi>](#) 11. Klimenko D.N., Kravtsov N.V., Lariontsev E.G., Firsov V.V. *Kvantovaya Elektron.*, **24**, 649 (1997) [*Quantum Electron.*, **27**, 631 (1997)].
- [doi>](#) 12. Klimenko D.N., Lariontsev E.G. *Kvantovaya Elektron.*, **25**, 369 (1998) [*Quantum Electron.*, **28**, 358 (1998)].
- [doi>](#) 13. Kravtsov N.V., Pashinin P.P., Sidorov S.S., Firsov V.V., Chekina S.N. *Kvantovaya Elektron.*, **33**, 321 (2003) [*Quantum Electron.*, **33**, 321 (2003)].
- [doi>](#) 14. Kravtsov N.V., Lariontsev E.G. *Kvantovaya Elektron.*, **30**, 105 (2000) [*Quantum Electron.*, **30**, 105 (2000)].
- [doi>](#) 15. Zolotoverkh I.I., Lariontsev E.G. *Kvantovaya Elektron.*, **23**, 620 (1996) [*Quantum Electron.*, **26**, 604 (1996)].
- [doi>](#) 16. Zolotoverkh I.I., Kravtsov N.V., Kravtsov N.N., Lariontsev E.G., Makarov A.A. *Kvantovaya Elektron.*, **24**, 638 (1997) [*Quantum Electron.*, **27**, 621 (1997)].
17. Polushkin N.I., Khandokhin P.A., Khanin Ya.I. *Kvantovaya Elektron.*, **10**, 1461 (1983) [*Sov. J. Quantum Electron.*, **13**, 950 (1983)].
- [doi>](#) 18. Zolotoverkh I.I., Klimenko D.N., Kravtsov N.V., Lariontsev E.G., Firsov V.V. *Kvantovaya Elektron.*, **23**, 938 (1996) [*Quantum Electron.*, **26**, 914 (1996)].
19. Haken H. *Lazernaya svetodinamika* (Laser Light Dynamics) (Moscow: Mir, 1998).
- [doi>](#) 20. Sanchz F., LeFlohic M., Stephan G.M., LeBoudec P., Fracois P.L. *IEEE J. Quantum Electron.*, **31**, 481 (1995).
- [doi>](#) 21. Kravtsov N.V., Lariontsev E.G. *Kvantovaya Elektron.*, **21**, 903 (1994) [*Quantum Electron.*, **24**, 841 (1994)].